

Theory of Trapped-Hole Centers in Aluminum Oxide*

R. H. BARTRAM, C. E. SWENBERG,† AND J. T. FOURNIER

The University of Connecticut, Storrs, Connecticut

(Received 8 March 1965)

Energy levels of trapped-hole centers in gamma- and reactor-irradiated Al_2O_3 are calculated in order to verify models proposed to account for some of the electron-spin resonance (ESR) spectra and to correlate these with optical-absorption spectra. Crystal-field theory is employed in the calculation of energy levels, including *a priori* calculation of the crystal field on the point-ion model. Lattice distortion by the defect is considered only qualitatively; nevertheless, a number of conclusions are possible. The calculated zero-field splitting of interstitial O^0 , which is 0.268 cm^{-1} without distortion and substantially larger with distortion, could account for the absence of an ESR spectrum at X band. A single optical band associated with this center is correlated with a measured band of 2.0 eV. Interstitial O^+ has a calculated zero-field splitting of 0.174 cm^{-1} without distortion, but outward displacement of the two nearest Al^{3+} ions by only 0.17 \AA accounts for the observed zero-field splitting of 0.074 cm^{-1} . No optical absorption is associated with this center. For O^- adjacent to a charge-deficient cation site, the assumption of a cation vacancy leads to an optical band at $\Delta = 2.93 \text{ eV}$ which correlates with an observed band at 3.08 eV. The calculated value of λ/Δ , where λ is the spin-orbit constant, is -0.0057 compared with the ESR value of -0.0073 .

I. INTRODUCTION

THE study of color centers by optical absorption measurements has proved to be a profitable approach to the investigation of radiation-induced defects in ionic crystals. The technique of electron-spin resonance (ESR) is employed in much the same way, often with the advantage that it provides more detailed information about the nature of the defects. Both of these techniques have been employed in the investigation of irradiated single crystals of α -aluminum oxide,¹⁻⁴ and qualitative features of the ESR spectra have suggested models for the radiation-induced defects and centers. The present paper is concerned with an effort to account quantitatively for the ESR spectra in order to verify these models, and to correlate the centers with the optical spectra.

Levy¹ has analyzed the spectra of gamma-irradiated and reactor-irradiated aluminum oxide into a number of Gaussian components by a curve-fitting procedure. The gamma-ray-induced spectrum was found to consist of prominent bands with peaks at 3.08 and 5.45 eV and a band of lesser intensity at 4.28 eV. The reactor-induced spectrum was resolved in two ways; the preferred resolution yielded bands with peaks at the following energies: 2.00, 2.64, 3.74, 4.21, 4.84, 5.34, and 6.02 eV. The intensity increased monotonically with photon energy, the band at 6.02 eV being considerably more prominent than the others. Mitchell, Rigden, and Townsend² resolved the spectra of reactor-irradiated aluminum oxide by means of the anisotropy of the optical absorption. Their results are in general agree-

ment with those of Levy. They report an isotropic band at 6.1 eV, bands of positive anisotropy at 2.8, 3.5, 4.1, and 4.8 eV, one band of negative anisotropy at 5.3 eV and at least one other at either 3.8 or 3.1 eV. (They define the anisotropy to be positive when light polarized parallel to the *c* axis is absorbed more strongly than light polarized perpendicular to the *c* axis.) In addition, they observe weak bands at 1.9 and 2.2 eV whose anisotropy they do not specify.

Gamble *et al.*³ have investigated the ESR spectra of gamma-irradiated Al_2O_3 . Gamma irradiation yields a single, asymmetric, anisotropic line which they interpret as the superposition of spectra tentatively attributed to *F* centers and to holes which are trapped at charge-deficient cation sites and localized on neighboring anions (i.e., O^- ions). The charge-deficient cation sites may be vacant or may contain monovalent or divalent cation impurities. The trapped holes have $g_{\parallel} = 2.006 \pm 0.003$ and $g_{\perp} = 2.020 \pm 0.003$, where \parallel and \perp are with respect to the line joining the O^- ion with the charge-deficient cation site.

Two ESR spectra result from reactor irradiation of Al_2O_3 .⁴ One is a large, single, asymmetric, anisotropic line which has not been resolved into components but which is clearly different from the gamma-ray induced absorption. The other is a well-resolved 12-line spectrum corresponding to a center with spin 1 in six inequivalent sites, which has been attributed to $(\text{AlO})^{\pm}$ -molecule ions formed by replacement collisions. Finally, when a reactor-irradiated sample is subjected to low-temperature gamma irradiation, a 3-line spectrum is produced. This spectrum corresponds to a center with spin $\frac{3}{2}$ in a site with axial symmetry about the crystal *c* axis, and is attributed to interstitial O^+ ions. It is inferred that these centers are formed from interstitial oxygen atoms, produced by reactor irradiation, whose ESR spectra are not observed, presumably because of large zero-field splitting. The spin-Hamiltonian parameters for the 3-line spectrum are $g_{\parallel} = 2.018 \pm 0.002$, $g_{\perp} = 2.011 \pm 0.002$, and $|D| = 0.037 \pm 0.001 \text{ cm}^{-1}$.

* This research was supported by the U. S. Atomic Energy Commission.

† Present address: University of Rochester, Rochester, N. Y.

¹ P. W. Levy, Phys. Rev. **123**, 1226 (1961).

² E. W. J. Mitchell, J. D. Rigden, and P. D. Townsend, Phil. Mag. **5**, 1013 (1960).

³ F. T. Gamble, R. H. Bartram, C. G. Young, O. R. Gilliam, and P. W. Levy, Phys. Rev. **134**, A589 (1964).

⁴ F. T. Gamble, R. H. Bartram, C. G. Young, O. R. Gilliam, and P. W. Levy, Phys. Rev. **138**, A577 (1965).

In this paper, theoretical models are developed for some of the possible trapped-hole centers in gamma-ray and reactor-irradiated aluminum oxide, and the corresponding optical-absorption-band energies and spin-Hamiltonian parameters are calculated. The defects considered are interstitial anions and charge-deficient cation sites. Centers formed by trapping two and three holes at an interstitial anion are investigated; these may be alternately characterized as interstitial O^0 and O^+ ions. The center associated with the charge-deficient cation site involves a single hole localized on an adjacent anion, or alternatively, an O^- ion in a normal anion site adjacent to a charge-deficient cation site. The trapped holes in aluminum oxide are believed to be well localized on individual anions, for reasons discussed in Sec. II, and accordingly a tight-binding approximation is indicated. The method employed is a literal application of the crystal-field theory developed by Bethe,⁵ Penney and Schlapp,⁶ and Van Vleck.⁷

Crystal-field theory has been used extensively and successfully in the interpretation of optical absorption and electron-spin-resonance data⁸; however, in these applications the strength of the crystal-field has been left as an adjustable parameter. Attempts to calculate the crystal field from first principles have been less successful. The model as originally conceived is that of a static potential field arising from an array of point charges or dipoles representing the ions other than the paramagnetic ion. This model should correspond most closely to the situation in ionic complexes, and was applied with apparent success by Van Vleck⁹ and Polder¹⁰ to salts of transition-metal ions. However, subsequent refinements¹¹⁻¹⁷ of the theory have destroyed the agreement with experiment, and effects due to exchange, overlap, covalency, and penetration of the ligand electron cloud were found to be comparable to the point-ion contribution. The more rigorous formulation of the problem by Jarret¹⁸ has not lent itself to calculations. Thus the range of validity of the point-ion model for the crystal field remains uncertain, and attempts to refine the model have so far failed.

In the present application there is insufficient data associated with each center to justify the inclusion of adjustable parameters, and it is therefore essential to attempt an *a priori* calculation of the crystal field.

Fortunately, for both of the defects considered, the configuration of ions about the defect is such as to favor the application of the point-ion model. At both the interstitial site and the normal anion site the nearest oxygen ions are arranged with sufficiently high symmetry that they make a negligible contribution to the relevant part of the crystal field. The contribution of the nearest aluminum ions is comparable with that of the rest of the lattice; however, the distance of the nearest aluminum ions from the defect site is approximately equal to the sum of the ionic radii of Al^{3+} and O^{2-} , while the ions occupying the defect sites are O^+ , O^0 , and O^- , with more compact wave functions than O^{2-} . It is therefore anticipated that in this case the contributions to the crystal field of the effects mentioned above,¹¹⁻¹⁷ which depend on the proximity of the paramagnetic ion and the ligands, may be small compared with the point-ion contribution. The proximity of the oxygens may indirectly affect the crystal-field splitting by expanding or compressing the $2p$ orbitals on the paramagnetic ion and consequently altering the value of $\langle r^2 \rangle$, which is the relevant parameter in this case. No allowance has been made for this effect, but it should be noted that $\langle r^2 \rangle$ is considerably less sensitive to the scale of the wave function than is $\langle r^4 \rangle$, which is the relevant parameter for transition metal ions. Also, no allowance has been made for changes in the spin-orbit coupling constant and free-ion-term separations.¹⁹

From the foregoing, it appears that an *a priori* calculation of the crystal field on the point-ion model is reasonable in the present application in spite of its apparent failure in ionic complexes of transition metal ions. However, since we are dealing with point defects which introduce a local distortion of the lattice, a calculation based on the undistorted lattice is inadequate. Artman and Murphy²⁰ have done a similar calculation for transition-metal impurities in Al_2O_3 in which they introduced a model for the local distortion which incorporates adjustable parameters; in their case the crystal field was substantially affected by distortion. Since no adjustable parameters are justified in the present case, what is needed is an *a priori* calculation of distortion along the lines of the treatment of Hatcher and Dienes²¹ for interstitial Cl^0 in $NaCl$. This calculation has not been carried out for Al_2O_3 and the effects of distortion are considered only qualitatively. In a sense, this procedure introduces an adjustable parameter; however, the parameter is not quite arbitrary in that we require the effect of distortion to be in the right direction and of reasonable magnitude. The effect of covalency within the Al_2O_3 structure, which would reduce the charges on the point ions, has not been considered explicitly since it is qualitatively similar to the effect of distortion.

⁵ H. Bethe, Ann. Physik 3, 133 (1929).
⁶ W. G. Penney and R. Schlapp, Phys. Rev. 41, 194 (1932).
⁷ J. H. Van Vleck, Phys. Rev. 41, 208 (1932).
⁸ William Low, *Paramagnetic Resonance in Solids*, Suppl. 2 of *Solid State Physics*, edited by F. Seitz and D. Turnbull (Academic Press Inc., New York, 1960).
⁹ J. H. Van Vleck, J. Chem. Phys. 7, 72 (1939).
¹⁰ D. Polder, Physica 9, 709 (1942).
¹¹ H. W. Kleiner, J. Chem. Phys. 20, 1784 (1952).
¹² J. C. Phillips, J. Phys. Chem. Solids 11, 226 (1959).
¹³ Y. Tanabe and S. Sugano, J. Phys. Soc. Japan 11, 864 (1956).
¹⁴ A. J. Freeman and R. E. Watson, Phys. Rev. 120, 1254 (1960).
¹⁵ S. Sugano and R. G. Shulman, Phys. Rev. 130, 517 (1963).
¹⁶ J. H. Van Vleck, J. Chem. Phys. 3, 803 (1935).
¹⁷ R. E. Watson and A. J. Freeman, Phys. Rev. 134, A1526 (1964).
¹⁸ H. S. Jarrett, J. Chem. Phys. 31, 1579 (1959).

¹⁹ J. Owen, Proc. Roy. Soc. (London) A227, 183 (1955).

²⁰ J. O. Artman and J. C. Murphy, Phys. Rev. 135, A1622 (1964).

²¹ R. D. Hatcher and G. J. Dienes, Phys. Rev. 134, A214 (1964).

Section II is devoted to calculation of the crystal field from the point-ion lattice model. In the following three sections this crystal field is employed in the calculation of energy levels of interstitial O^0 , interstitial O^+ , and O^- adjacent to a charge-deficient cation site.

II. CRYSTAL FIELD

The aluminum-oxide structure can be viewed as a slight distortion from hexagonal close packing of O^{2-} ions with Al^{3+} ions occupying two out of three interstices. The remaining interstices appear as natural voids in the crystal, and invite speculation that they are the ultimate resting places of some of the ions displaced by fast neutrons. If the oxygen ions are viewed as hard spheres with radius equal to the ionic radius, 1.40 Å,²² then the interstitial site can accommodate an ion of radius 0.58 Å. The appropriate radius of O^0 and O^+ in the present context may be somewhat larger than this; nevertheless, it appears that O^0 and O^+ can be incorporated interstitially with relatively small distortion, and consequently that a tight-binding approximation is justified. The orbits of electrons trapped at interstitial aluminum ions could not be accommodated in the void and because of the high dielectric constant would presumably extend over many ion sites. For that reason these centers are not dealt with in the present paper. The O^- ion next to a charge-deficient cation site can also be treated by the tight-binding method, since it occupies an anion site with radius 1.40 Å.

One step in the crystal-field calculation is the determination of the electrostatic potential at the interstitial site due to the rest of the crystal regarded as a rigid array of point ions. The potential $V(\mathbf{r})$ in the region occupied by the interstitial ion is given by

$$V(\mathbf{r}) = \sum_{l=0}^{\infty} \sum_{m=0}^l r^l P_l^m(\cos\theta) \times [c_{lm} \cos m\phi + d_{lm} \sin m\phi], \quad (\text{II.1})$$

where

$$c_{lm} = \sum_{\alpha} \frac{q_{\alpha}}{r_{\alpha}^{l+1}} (2 - \delta_{m0}) \frac{(l-m)!}{(l+m)!} \times P_l^m(\cos\theta_{\alpha}) \cos m\phi_{\alpha}, \quad (\text{II.2a})$$

$$d_{lm} = \sum_{\alpha} \frac{q_{\alpha}}{r_{\alpha}^{l+1}} (2 - \delta_{m0}) \frac{(l-m)!}{(l+m)!} \times P_l^m(\cos\theta_{\alpha}) \sin m\phi_{\alpha}. \quad (\text{II.2b})$$

In Eqs. (II.2), q_{α} is the charge on the α th ion and \mathbf{r} is its position with respect to the center of the interstitial site.

Equations (II.2) can be used to evaluate the electrostatic potential at the interstitial site. However, it has

²² W. H. Zachariasen, *Z. Krist.* **80**, 137 (1931).

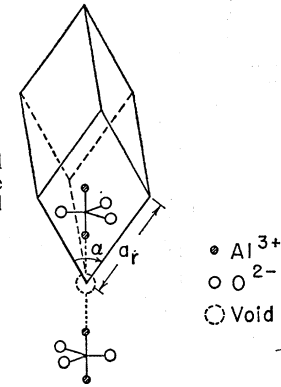


FIG. 1. A primitive unit cell and basis of the corundum lattice. The dimensions are $a_r = 5.124$ Å and $\alpha = 55^\circ 17'$.

been pointed out by Evjen²³ that in order to ensure rapid convergence of lattice sums of this type, it is essential to divide the lattice into symmetrical units which possess only high-order multipole moments.²⁴ When the distortion from hexagonal close packing is considered, $\alpha\text{-Al}_2\text{O}_3$ is trigonal with space group D_{3d}^6 . The rhombohedral unit cell and basis are illustrated in Fig. 1. The symmetrical unit assembly which was chosen for the evaluation of the electrostatic potential at the interstitial site consisted of ten ions in the two "molecules" associated with each lattice point, as shown in Fig. 2.

The number of constants c_{lm} and d_{lm} which must be calculated is limited by symmetry; the point symmetry at the interstitial site is C_{3i} , and the only nonvanishing constants are those for which l is even and m is a multiple of 3. Since we will only consider p orbitals, the sum in Eq. (II.1) can be truncated after $l=2$, and the crystal field can be characterized by a single parameter, c_{20} .

For one of the centers, O^- adjacent to a charge-deficient cation site, it was necessary to evaluate the crystal potential at an anion site with point symmetry C_2 . The significant parameters at the anion site are c_{20} , c_{22} , and d_{22} .

The coordinates of the ions in a unit assembly were

TABLE I. Coordinates of the ions in a unit assembly in units of a_r . The origin of coordinates is at the interstitial site, and the axes are oriented as shown in Fig. 2.

| ion | x | y | z |
|-----|---------|---------|---------|
| 1 | 0 | 0 | 0.3750 |
| 2 | 0.2457 | 0.1418 | 0.6334 |
| 3 | -0.2457 | 0.1418 | 0.6334 |
| 4 | 0 | -0.2837 | 0.6334 |
| 5 | 0 | 0 | 0.8918 |
| 6 | 0 | 0 | -0.3750 |
| 7 | -0.2457 | -0.1418 | -0.6334 |
| 8 | 0.2457 | -0.1418 | -0.6334 |
| 9 | 0 | 0.2837 | -0.6334 |
| 10 | 0 | 0 | -0.8918 |

²³ H. M. Evjen, *Phys. Rev.* **39**, 675 (1932).

²⁴ J. Kanamori, T. Moriya, K. Motizuki, and T. Nagamiya, *J. Phys. Soc. Japan* **10**, 93 (1955).

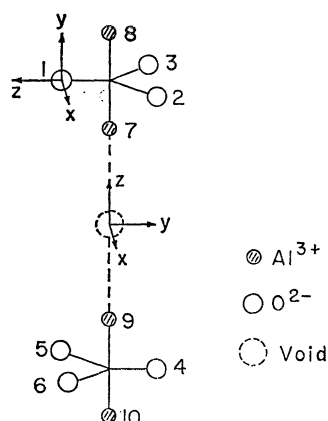


FIG. 2. Symmetrical unit assembly chosen to ensure convergence of lattice sums. The ions are numbered for future reference, and coordinate systems required for the specification of the constants in the potential expansions are defined at the void and at anion site 1.

calculated from the lattice dimensions given by Newnham and de Haan,²⁵ and are listed in Table I. The crystal-field constants were calculated from Eqs. (II.2) and are listed in Table II. Different coordinate systems were used for the interstitial site and anion site as shown in Fig. 2. The signs of the constants for the anion site are those appropriate to ion 1 of Fig. 2. The lattice sum was extended over all unit assemblies whose centers were within a sphere of specified radius from the interstitial site. Two different spheres were used: one of radius $3.1a_r$, where a_r is the edge length of the rhombohedral unit cell given in Fig. 1, containing 189 unit assemblies; and one of radius $4.1a_r$ containing 447 unit assemblies. It can be seen from Table II that the additional unit assemblies in the larger sphere make a very small contribution to the constants, the difference being greatest for c_{00} as expected. The values of the constants employed in the crystal-field calculations are those obtained with the larger sphere.

Similar calculations have been carried out for the aluminum site in $\alpha\text{-Al}_2\text{O}_3$ and the chromium site in ruby by Artman and Murphy,²⁰ who point out that because of the low symmetry there are electric fields at both the aluminum and oxygen sites which induce dipole moments, and that these dipole moments make

TABLE II. Crystal-field constants in Al_2O_3 at the interstitial site, oxygen site, and aluminum site. The coordinate axes are as shown in Fig. 2, and the signs of the constants for the oxygen site are appropriate to ion 1 of Fig. 2. The lattice sums were carried out over spheres of radius $3.1a_r$ and $4.1a_r$. The constants c_{lm} and d_{lm} are expressed in units of e/a_r^{l+1} .

| Site | Constant | $3.1a_r$ | $4.1a_r$ |
|--------------|----------|----------|----------|
| Interstitial | c_{00} | -0.354 | -0.564 |
| | c_{20} | 77.920 | 77.922 |
| Oxygen | c_{00} | 10.106 | 9.897 |
| | c_{20} | 11.096 | 11.089 |
| | c_{22} | 0.263 | 0.259 |
| | d_{22} | -16.518 | -16.519 |
| Aluminum | c_{00} | -12.320 | -12.529 |

²⁵ R. E. Newnham and Y. M. de Haan, *Z. Kristall.* **117**, 235 (1962).

a contribution to the crystal-field parameters. The dipole moments reported by Artman and Murphy were verified and their contributions to the crystal-field constants at both interstitial and anion sites were calculated. It was found that the effect of the dipole moments at these two sites is very small; accordingly, the dipole contribution is not included in Table II.

Finally, values of c_{00} at the aluminum site, oxygen site, and interstitial site were calculated and are also listed in Table II. While the sums are conditionally convergent, the differences between them are absolutely convergent (it is for this reason that the Madelung constant can be specified uniquely). The choice of a spherical array of molecules is a natural one in this case, because the contributions of remote quadrupole moments cancel and the potential is due entirely to nearby ions. It is seen that the potential at the interstitial site is intermediate between the potentials at the cation and anion sites, and is nearly zero. Thus the presence of an interstitial ion of either sign has little effect on the electrostatic energy of the lattice, with the consequence that interstitial O^0 and O^+ are *a priori* equally plausible.

III. INTERSTITIAL O^0

The optical absorption energies and spin-Hamiltonian parameters of interstitial O^0 are determined from the Hamiltonian

$$\mathcal{H} = W_F + V_C + \Lambda + W_H, \quad (\text{III.1})$$

where W_F has the form

$$W_F = \sum_i (-\hbar^2/2m)\nabla_i^2 - Ze^2/r_i + \sum_{j>i} \frac{e^2}{r_{ij}}, \quad (\text{III.2})$$

V_C is the potential energy due to the crystal field,

$$V_C = \sum_i -eV(\mathbf{r}_i), \quad (\text{III.3})$$

Λ is the spin-orbit interaction, and W_H is the Zeeman interaction with the external field. The terms W_F and V_C taken together constitute the optical Hamiltonian \mathcal{H}_O ,

$$\mathcal{H}_O = W_F + V_C. \quad (\text{III.4})$$

The eigenvalues of \mathcal{H}_O are the optical energy levels. We regard V_C as comparable to the electrostatic interaction of the electrons. The procedure is essentially that employed by Finkelstein and Van Vleck²⁶ and Orgel²⁷ in the case of iron-group transition metals, except that the crystal field is not regarded as a parameter but is calculated from the point-ion lattice model as described in Sec. II.

The first excited configuration of W_F , $2s^2 2p^3 3s$, lies $74,000 \text{ cm}^{-1}$ above the ground configuration, $2s^2 2p^4$, according to Moore.²⁸ In the crystal, this separation is

²⁶ R. Finkelstein and J. H. Van Vleck, *J. Chem. Phys.* **8**, 790 (1940).

²⁷ L. E. Orgel, *J. Chem. Phys.* **23**, 1004 (1955).

²⁸ C. E. Moore, U. S. Natl. Bur. Std. Circular No. 467, (1949).

TABLE III. (a) Matrix elements of the crystal potential within the ground configuration of interstitial O⁰.
(b) Corresponding eigenvalues. The parameter γ is defined by $\gamma = (1/5)ec_{20}\langle r^2 \rangle$.

| (a) | | (b) |
|-----|---|--|
| A: | $\begin{matrix} {}^1S & & {}^1D \\ \hline {}^1S & \begin{vmatrix} E_S & 2\sqrt{2}\gamma \\ 2\sqrt{2}\gamma & E_D+2\gamma \end{vmatrix} \\ {}^1D & \end{matrix}$ | $\begin{matrix} \frac{1}{2}(E_S+E_D+2\gamma) + [\frac{1}{4}(E_S-E_D-2\gamma)^2+8\gamma^2]^{1/2} \\ \frac{1}{2}(E_S+E_D+2\gamma) - [\frac{1}{4}(E_S-E_D-2\gamma)^2+8\gamma^2]^{1/2} \end{matrix}$ |
| | $\begin{matrix} {}^3P \\ \hline {}^3P \parallel E_P-2\gamma \parallel \end{matrix}$ | $E_P-2\gamma$ |
| E: | $\begin{matrix} {}^1D & & {}^1D \\ \hline {}^1D & \begin{vmatrix} E_D+\gamma & 0 \\ 0 & E_D-2\gamma \end{vmatrix} \\ {}^1D & \end{matrix}$ | $\begin{matrix} E_D+\gamma \\ E_D-2\gamma \end{matrix}$ |
| | $\begin{matrix} {}^3P \\ \hline {}^3P \parallel E_P+\gamma \parallel \end{matrix}$ | $E_P+\gamma$ |

probably increased since the 3s wave function extends into a region of high dielectric constant. Since this energy exceeds the band gap in Al₂O₃,²⁹ only transitions within the ground configuration are expected to contribute to the observed optical absorption spectrum.

The matrix elements of V_C were calculated within the ground configuration in a representation in which W_F is diagonal; this procedure had the advantage that the empirically determined term energies of the free atom could be used for the eigenvalues of W_F . The eigenfunctions of W_F were obtained as combinations of Slater determinants by the method of Condon and Shortley.³⁰ The calculation of matrix elements was facilitated by the use of an equivalent operator for the crystal potential³¹; within the ground configuration, V_C can be replaced by

$$V_C = (\frac{1}{5})ec_{20}\langle r^2 \rangle \sum_i [3l_{zi}^2 - l_i(l_i+1)], \quad (III.5)$$

where c_{20} is the crystal-field parameter discussed in Sec. II, and $\langle r^2 \rangle$ denotes the radial integral

$$\langle r^2 \rangle = \int_0^\infty P^2(2p|r)r^2 dr, \quad (III.6)$$

where $P(2p|r)/r$ is the radial part of a 2p orbital for O⁰.

The diagonalization of the matrix of V_C is greatly simplified by the fact that the functions $|LM_LSM_S\rangle$ transform as basis functions for irreducible representations Γ of C_3 (all functions are even under inversion, which is not considered further). The correspondence between M_L and Γ is as follows: Functions with $M_L=3n$ belong to the A representation, and those with $M_L=3n+1$ and $M_L=3n+2$ to the E representation. Since V_C transforms like the identity representation of C_3 , there can be no matrix elements connecting states with different Γ 's. Also, there are no matrix elements connecting states of different S or M_S , since V_C operates

²⁹ R. Bauple, A. Gilles, J. Ramand, and B. Vodar, J. Opt. Soc. Am. **40**, 788 (1950).

³⁰ E. V. Condon and G. H. Shortley, *The Theory of Atomic Spectra* (Cambridge University Press, Cambridge, England, 1959), p. 226.

³¹ K. W. H. Stevens, Proc. Phys. Soc. (London) **A65**, 209 (1952).

only on the space coordinates. The matrices to be diagonalized are shown in Table III. It can be seen that only the ¹SA and ¹DA states are mixed by the perturbation; the eigenvalues of the resulting 2x2 matrix are also listed. Here, V_C has been expressed in units of γ defined by

$$\gamma = (\frac{1}{5})ec_{20}\langle r^2 \rangle, \quad (III.7)$$

while E_S , E_D and E_P are the eigenvalues of W_F . The crystal-field parameter c_{20} is listed in Table II as $c_{20}=77.922 e/a_r^3$. The quantity $\langle r^2 \rangle$ was evaluated by carrying out the integration in Eq. (III.6) numerically, using a 2p wave function calculated by Hartree, Hartree, and Swirls.³² Strictly speaking, this wave function is appropriate only to the ³P term, since it was obtained by the Hartree-Fock procedure for that term, while we are committed to the point of view that the one-electron orbitals are uniquely determined by the configuration. However, the differences between the wave functions for different terms of the ground configuration are very slight, and may be neglected in view of the uncertainty in c_{20} . The value of $\langle r^2 \rangle$ in atomic units was found to be

$$\langle r^2 \rangle = 1.98. \quad (III.8)$$

The energy levels of the optical Hamiltonian \mathcal{H}_O were calculated from Table III together with Eqs. (III.7)

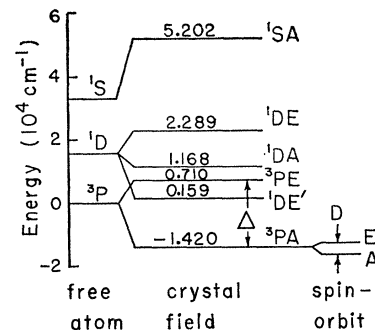


FIG. 3. Energy levels of interstitial O⁰ in Al₂O₃ calculated for the undistorted lattice. The zero-field splitting of the spin degeneracy is not drawn to scale.

³² D. R. Hartree, W. Hartree, and B. Swirls, Phil. Trans. Roy. Soc. **A238**, 229 (1939).

and (III.8) and the empirical term energies of the free atom,²⁸ and are shown in Fig. 3.

In spite of the fact that the interstitial site is a center of inversion, the parity selection rule can be upset by lattice vibrations.³³ Transitions between states of different multiplicity are more strongly forbidden, however. Thus only a single optical-absorption band is expected from this center, corresponding to a transition between the 3PA and 3PE levels, at $21,300\text{ cm}^{-1}$ or 2.63 eV .

The terms $\Lambda + W_H$ in Eq. (III.1) split the spin degeneracy of the ground term of \mathcal{H}_O , and the ESR spectrum arises from transitions between the resulting energy levels. Pryce³⁴ has shown that, for the case in which the ground term of \mathcal{H}_O is orbitally nondegenerate and V_C is small compared with the term separation, the energy levels arising from the ground term are given approximately by the unperturbed energy plus the eigenvalues of the spin Hamiltonian,

$$\mathcal{H}_S = \beta \mathbf{H} \cdot \mathbf{g} \cdot \mathbf{S} - \lambda^2 \mathbf{S} \cdot \mathbf{A} \cdot \mathbf{S}. \quad (\text{III.9})$$

In Eq. (III.9) \mathbf{H} is the magnetic field intensity, \mathbf{S} is the spin angular-momentum operator, β is the Bohr magneton, and \mathbf{g} and \mathbf{A} are tensor quantities given by

$$\mathbf{g} = 2.0023(1 - \lambda \mathbf{A}), \quad (\text{III.10a})$$

$$\mathbf{A} = \sum_{n>0} \langle 0 | \mathbf{L} | n \rangle \langle n | \mathbf{L} | 0 \rangle / (E_n - E_0), \quad (\text{III.10b})$$

where \mathbf{L} is the orbital angular-momentum operator and the sum is extended over the levels E_n of $W_F + V_C$ which arise from the ground term of W_F . Equations (III.9) and (III.10) were employed in the calculation of spin-Hamiltonian parameters; i.e., only states arising from the 3P term of W_F were considered. This procedure is not entirely justified in view of the fact that V_C is comparable to the electrostatic interaction. However, it is better than it seems for the following reason: There are no matrix elements of the spin-orbit interaction which connect the 3PA and ${}^1DE'$ terms of \mathcal{H}_O , since the corresponding basis functions have different values of M_J . Also, the separation between the 1DE and 1DA levels is small compared with their separation from the 3PA level, with the consequence that their contribution to the zero-field splitting of the spin degeneracy is small. Thus the major contribution to the zero-field splitting comes from the 3PE level.

In the present application, Eq. (III.9) reduces to

$$\mathcal{H}_S = g_1 \beta (H_x S_x + H_y S_y) + g_{11} \beta H_z S_z + D [S_z^2 - \frac{1}{3} S(S+1)], \quad (\text{III.11})$$

where

$$g_{11} = 2.0023, \quad (\text{III.12a})$$

$$g_1 = 2.0023(1 - \lambda/\Delta), \quad (\text{III.12b})$$

$$D = \lambda^2/\Delta, \quad (\text{III.12c})$$

$$\Delta \equiv E({}^3PE) - E({}^3PA), \quad (\text{III.12d})$$

the z axis is taken parallel to the crystal c axis, and a constant term has been omitted. Using the value of Δ derived previously, $21,300\text{ cm}^{-1}$, and a value of λ derived from Moore's tables²⁸ by taking $\frac{1}{3}$ the total width of the ground multiplet, -75.5 cm^{-1} , we obtain

$$g_1 = 2.0090, \quad (\text{III.13a})$$

$$D = 0.268\text{ cm}^{-1}. \quad (\text{III.13b})$$

The parameter D is also the zero-field splitting, as can be seen from Eq. (III.11) with $S=1$.

The value of D given by Eq. (III.13b) is appropriate to a rigid lattice, undistorted by the interstitial ion. We now consider qualitatively the effect of distortion. It can be seen from Table III that $\Delta = 3\gamma$. It follows from Eqs. (III.7) and (III.12c) that D is given by

$$D = 5\lambda^2/3ec_{20}\langle r^2 \rangle, \quad (\text{III.14})$$

and therefore the zero-field splitting is inversely proportional to the crystal-field parameter c_{20} . The contributions of the ions immediately surrounding the interstitial site were calculated. In units of e/a_r^3 , the contribution of the two nearest Al^{3+} ions is 113.778 , while that of the nearest six O^{2-} ions is 11.951 , for a total of 125.729 . The contribution of the rest of the lattice must then be -47.807 . It can be seen from Eq. (II.2a) that the contribution of each ion to c_{20} is inversely proportional to the cube of its distance from the interstitial site, provided its orientation is fixed. Consider an oversimplified model of the distortion in which the eight neighboring ions are displaced radially by a fixed fraction of their original distance in order to accommodate the interstitial ion, while the rest of the lattice remains rigid. From the foregoing considerations, it can be seen that a 38% increase in the distance of the neighboring ions from the void would reduce their contribution to c_{20} to the extent that it would just cancel the contribution of the rest of the lattice. The void could then accommodate an ion of radius 1.33 \AA , compared with 0.58 \AA for the undistorted lattice. Thus the crystal field is seen to be extremely sensitive to distortion, and a relatively small dilation of the void would decrease c_{20} substantially with a corresponding increase in D . The energy of the microwave photons employed in the ESR measurements was 0.3 cm^{-1} , only slightly larger than the value of D calculated for the rigid lattice. The distortion could easily make the zero-field splitting exceed the photon energy to the extent that no ESR spectrum could be observed. [It is evident from Eq. (III.11) that with $D > 0$, a spin singlet lies lowest.]

While the value of Δ calculated for the rigid lattice, 2.63 eV , agrees well with the energy of a band observed by Mitchell, Rigden, and Townsend² at 2.8 eV and by Levy¹ at 2.64 eV , it should be noted that the distortion which increases D correspondingly diminishes Δ . Thus a more likely identification is with one of the two bands observed by Mitchell *et al.*² at 1.9 and 2.2 eV , of un-

³³ J. H. Van Vleck, *J. Phys. Chem.* **41**, 67 (1937).

³⁴ M. H. L. Pryce, *Proc. Phys. Soc. (London)* **A63**, 25 (1950).

specified anisotropy, which were reported by Levy¹ as a single band at 2.0 eV. This alternative is substantiated by consideration of the anisotropy. The component of the electric-dipole-moment operator parallel to the crystal c axis transforms like the A representation of C_3 , and consequently light polarized parallel to the c axis could not induce the transition between the 3PA and 3PE levels, since the Kronecker product $A \times E = E$. On the other hand, the transverse components transform like E , so light polarized perpendicular to the c axis can be absorbed. (Here, the parity selection rule is assumed inoperative.) Therefore the anisotropy of the band produced by interstitial O^0 should be negative, whereas that of the 2.8-eV band was observed to be positive.

IV. INTERSTITIAL O^+

The optical absorption energies and spin-Hamiltonian parameters for interstitial O^+ cannot be found by the method used in Sec. III for interstitial O^0 , since all matrix elements of the spin-orbit interaction vanish within the 4S ground term. Nevertheless, the spin degeneracy is not required by symmetry and will therefore be removed in some higher order of perturbation theory.

The problem of zero-field splitting of S -state transition-metal ions has been investigated extensively.³⁵⁻³⁷ Van Vleck and Penney³⁵ and Watanabe³⁶ have considered the higher order perturbations responsible for the zero-field splitting in salts of Mn^{2+} and Fe^{3+} , and Gabriel, Johnston and Powell³⁷ successfully calculated the zero-field splitting of Mn^{2+} in cubic fields by diagonalizing the Hamiltonian, including spin interactions, within the ground configuration. This is essentially the approach employed here for interstitial O^+ .

The Hamiltonian is given by Eq. (III.1). However, Λ is enlarged to incorporate spin-spin interaction, which must be included since it may contribute to the zero-field splitting in a lower order of perturbation theory than the spin-orbit interaction; thus

$$\Lambda = \sum_i \xi_i \mathbf{l}_i \cdot \mathbf{s}_i + g^2 \beta^2 \sum_{j>i} \left[\frac{\mathbf{s}_i \cdot \mathbf{s}_j}{r_{ij}^3} - \frac{3(\mathbf{s}_i \cdot \mathbf{r}_{ij})(\mathbf{s}_j \cdot \mathbf{r}_{ij})}{r_{ij}^5} \right]. \quad (\text{IV.1})$$

The procedure for calculating the zero-field splitting then consists of diagonalizing the matrix of $W_F + V_C + \Lambda$ within the ground configuration. Gabriel, Johnston, and Powell³⁷ treated Λ as a perturbation on the optical Hamiltonian; in the present case, the matrices are of tractable size and it is feasible to perform the diagonalization exactly.

The ground configuration of the free O^+ ion contains the terms 4S , 2D , and 2P ; thus the matrix to be diagonalized is 20×20 . However, the matrix can be partitioned into smaller blocks by choosing as a basis combinations of zero-order wave functions which transform according to irreducible representations of double group C_3 (In this case, all functions are odd under inversion).

It was established that the original functions $|LM_L S M_S\rangle$ have the required transformation properties, and can be assigned to representations of C_3 and double group C_3 according to the quantum numbers M_L and M_J modulo 3, respectively.

Symmetry still allows off-diagonal elements of \mathcal{H} between states with M_J values differing by 3. However, a further simplification results from the fact that within the ground configuration V_C can be replaced by the equivalent operator given in Eq. (III.5). Consequently, V_C is diagonal in M_L as well as M_S ; also, Λ is diagonal in M_J . It follows that \mathcal{H} is diagonal in M_J and can thus be partitioned into two 1×1 , two 4×4 and two 5×5 blocks. Furthermore, it follows from time-reversal invariance that matrices corresponding to $\pm M_J$ have identical eigenvalues; thus we need only consider the three matrices for $M_J > 0$.

The matrix elements of W_F , which is diagonal in the chosen representation, were obtained from Moore's tables³⁸ by taking the average energy of each multiplet, and are given by $E_P = 40,467.4 \text{ cm}^{-1}$, $E_D = 26,816.8 \text{ cm}^{-1}$, and $E_S = 0$. The matrix elements of V_C were calculated by the method of Sec. III, using Eq. (III.5). Matrix elements of Λ have been calculated by Aller, Ufford, and Van Vleck³⁸ for O^+ in an $|LSJM_J\rangle$ representation in terms of two parameters, ζ and η , defined by

$$\zeta \equiv \frac{-e\hbar^2}{2m^2c^2} \int_0^\infty r^{-1} \frac{dV}{dr} P^2(2p|r) dr, \quad (\text{IV.2})$$

$$\eta \equiv \frac{e^2\hbar^2}{4m^2c^2} \int_0^\infty \int_0^{r_2} r_2^{-3} P^2(2p|r_1) P^2(2p|r_2) dr_1 dr_2. \quad (\text{IV.3})$$

Aller *et al.* obtained the values $\zeta = 174 \text{ cm}^{-1}$ and $\eta = 1.33 \text{ cm}^{-1}$. These values were later refined by Blume and Watson,³⁹ who obtained $\zeta = 172 \text{ cm}^{-1}$ and $\eta = 1.55 \text{ cm}^{-1}$. We have transformed the matrix of Λ to an $|LM_L S M_S\rangle$ representation and have used the values of ζ and η calculated by Blume and Watson. The three matrices to be diagonalized are shown in Table IV. The difference between the lowest eigenvalues of the $M_J = \frac{3}{2}$ matrix and the $M_J = \frac{1}{2}$ matrix is then the zero field splitting of the 4S term. In zero field, the spin Hamiltonian has the form

$$\mathcal{H}_S = D[S_z^2 - \frac{1}{3}S(S+1)]. \quad (\text{IV.4})$$

It follows that the zero-field splitting is $2D$.

The matrix elements of V_C are expressed in terms of the parameter γ defined by Eq. (III.7). The quantity

³⁵ J. H. Van Vleck and W. G. Penney, *Phil. Mag.* **17**, 961 (1934).

³⁶ H. Watanabe, *Progr. Theoret. Phys. (Kyoto)* **18**, 405 (1957).

³⁷ J. R. Gabriel, D. F. Johnston, and M. J. D. Powell, *Proc. Roy. Soc. (London)* **A264**, 503 (1961).

³⁸ L. H. Aller, C. W. Ufford, and J. H. Van Vleck, *Astrophys. J.* **109**, 42 (1949).

³⁹ M. Blume and R. E. Watson, *Proc. Roy. Soc. (London)* **A271**, 565 (1963).

TABLE IV. Matrix of $W_F + V_C + A$ within the ground configuration in an $|LM_LSM_S\rangle$ representation. The matrices are partitioned into blocks labeled by M_J , and only those blocks for $M_J > 0$ are shown. The rows and columns are labeled in the notation $^{2S+1}L(M_LM_S)$.

| $M_J = 5/2$ | | | | | |
|--|------------------------|------------------------|------------------------|------------------------|------------------------|
| ${}^2D(2\frac{1}{2}) \parallel E_D - 37\eta/5 \parallel$ | | | | | |
| $M_J = 3/2$ | ${}^2D(1\frac{1}{2})$ | ${}^2D(2-\frac{1}{2})$ | ${}^2P(1\frac{1}{2})$ | ${}^4S(0\frac{3}{2})$ | |
| ${}^2D(1\frac{1}{2})$ | $E_D - 37\eta/10$ | $-37\eta/5$ | $3\gamma + \xi/2$ | $-6\eta/5$ | |
| ${}^2D(2-\frac{1}{2})$ | $-37\eta/5$ | $E_D + 37\eta/5$ | $-\xi$ | $12\eta/5$ | |
| ${}^2P(1\frac{1}{2})$ | $3\gamma + \xi/2$ | $-\xi$ | $E_P - 5\eta/2$ | ξ | |
| ${}^4S(0\frac{3}{2})$ | $-6\eta/5$ | $12\eta/5$ | ξ | E_S | |
| $M_J = 1/2$ | | | | | |
| $M_J = 3/2$ | ${}^2D(0\frac{1}{2})$ | ${}^2D(1-\frac{1}{2})$ | ${}^2P(0\frac{1}{2})$ | ${}^2P(1-\frac{1}{2})$ | ${}^4S(0\frac{1}{2})$ |
| ${}^2D(0\frac{1}{2})$ | E_D | $-37(\sqrt{6})\eta/10$ | $\xi/\sqrt{3}$ | $\xi/\sqrt{6}$ | $-6\sqrt{2}\eta/5$ |
| ${}^2D(1-\frac{1}{2})$ | $-37(\sqrt{6})\eta/10$ | $E_D + 37\eta/10$ | $-\xi/\sqrt{2}$ | $3\gamma - \xi/2$ | $6\sqrt{3}\eta/5$ |
| ${}^2P(0\frac{1}{2})$ | $\xi/\sqrt{3}$ | $-\xi/\sqrt{2}$ | E_P | $-5\eta/\sqrt{2}$ | $\sqrt{2}\xi/\sqrt{3}$ |
| ${}^2P(1-\frac{1}{2})$ | $\xi/\sqrt{6}$ | $3\gamma - \xi/2$ | $-5\eta/\sqrt{2}$ | $E_P + 5\eta/2$ | $\xi/\sqrt{3}$ |
| ${}^4S(0\frac{1}{2})$ | $-6\sqrt{2}\eta/5$ | $6\sqrt{3}\eta/5$ | $\sqrt{2}\xi/\sqrt{3}$ | $\xi/\sqrt{3}$ | E_S |

$\langle r^2 \rangle$ was again evaluated by numerical integration using a $2p$ wave function for O^+ calculated by Hartree, Hartree, and Swirles,⁵⁴ with the result, in atomic units,

$$\langle r^2 \rangle = 1.46. \quad (\text{IV.5})$$

Using the value of c_{20} listed in Table II for the undistorted lattice, we obtain for γ the value

$$\gamma = 5,235 \text{ cm}^{-1}. \quad (\text{IV.6})$$

However, the positive charge of the interstitial ion would be expected to repel the two nearest cations which make the major contribution to this crystal field. Thus the value of γ appropriate to the distorted lattice should be smaller than the value given by Eq. (IV.6). Accordingly, the zero-field splitting was calculated for a range of values of γ . The spin-Hamiltonian parameter D is plotted in Fig. 4, and is seen to depend nearly quadratically on γ . The value of $|D|$ appropriate to the undistorted lattice is 0.087 cm^{-1} , which is more than twice the experimental value of 0.037 cm^{-1} . On the other hand, the value of γ corresponding to the experimental value of $|D|$ is 3550 cm^{-1} , a reduction of only

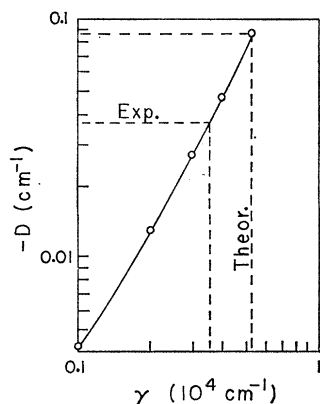


FIG. 4. Calculated spin-Hamiltonian parameter D as a function of γ for interstitial O^+ in Al_2O_3 , where γ is proportional to the strength of the crystal field.

32% from that for the undistorted lattice. In accordance with the discussion of lattice distortion in Sec. III, if this reduction is attributed entirely to a displacement of the two neighboring Al^{3+} ions, then their distance from the void is increased by just 9%, a displacement of 0.17 \AA . Thus the theory appears adequate to account for the observed ESR spectrum when allowance is made for the effect of lattice distortion.

The energy levels of the optical Hamiltonian given by Eq. (III.4) were calculated by diagonalizing the matrix of $W_F + V_C$ within the ground configuration, using the value $\gamma = 3550 \text{ cm}^{-1}$ which corresponds to the experimental value of $|D|$. The resulting energy levels are shown in Fig. 5. It can be seen that the crystal-field splitting of the 2D term is substantially less than its separation from the 4S term; this would be true for the value of γ appropriate to the undistorted lattice as well. Thus the 4S term remains the ground term, as it must to give a 3-line ESR spectrum, and electric-dipole transitions to the excited terms are forbidden by the change in multiplicity in addition to the parity selection rule. Consequently, it is anticipated that there will be no optical-absorption bands associated with interstitial O^+ which are of intensity comparable to that of the bands associated with other centers. This prediction has not yet been verified experimentally.

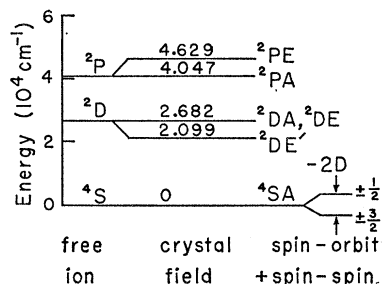


FIG. 5. Energy levels of interstitial O^+ in Al_2O_3 , calculated for $\gamma = 3550 \text{ cm}^{-1}$ which corresponds to the experimental value of $|D|$. The zero-field splitting of the spin degeneracy is not drawn to scale.

The eigenvectors of the Hamiltonian $W_F + V_C + A$ were also calculated, and matrix elements of the Zeeman energy W_H were calculated in this representation in an effort to account for the departure of the g values from the free-electron value. However, it was found that the Δg 's calculated were two orders of magnitude smaller than the experimental values. Thus it appears that configuration mixing must be considered in order to account for the observed g values.

An alternative approach to the calculation of zero-field splitting of an ion with configuration $1s^2 2s^2 2p^3$ has been developed by Chakravarty and Bersohn.⁴⁰ Their theory differs in two essential features from that employed here. First, they neglect spin-orbit interaction and attribute the entire zero-field splitting to spin-spin interaction, whereas in our calculation it was found that with γ given by Eq. (IV.6), spin-orbit interaction alone contributes 86% of the zero-field splitting. Second, they modify the $2p$ orbitals to include radial and angular excitations. These excitations are equivalent to configuration mixing which is neglected in our treatment. Chakravarty and Bersohn choose as their example atomic nitrogen in KN_3 , detected by Wylie *et al.*⁴¹ However, their results are readily adapted to the isoelectronic O^+ . Their parameter $t = (Z - s)/2$ is readily found to have the value 2.45 for O^+ by application of Slater's rules.⁴² They use a parameter q as a measure of the axial field which is related to our c_{20} by

$$q = -2c_{20}. \quad (\text{IV.7})$$

The spin-Hamiltonian parameter D can then be found from Fig. 1 of Ref. 40. When the value of c_{20} corresponding to the undistorted lattice is used in Eq. (IV.7), the value of D obtained is -0.0084 cm^{-1} . This is smaller than the experimental value by a factor of 4, and allowance for lattice distortion only increases the discrepancy. Thus it appears that the theory of Chakravarty and Bersohn is inadequate to account for the zero-field splitting of interstitial O^+ in Al_2O_3 ; in particular, spin-orbit interaction plays an essential role.

V. HOLE TRAPPED AT A CHARGE-DEFICIENT CATION SITE

It was noted in the introduction that the hole trapped at a charge-deficient cation site is localized on a neighboring anion. Thus the center may be regarded as an O^- ion in an anion site subject to the normal crystal field at that site together with the field due to the charge deficiency at the cation site. The method employed in Sec. III for the calculation of the optical levels and spin-Hamiltonian parameters for interstitial O^0 is applicable to this center as well. The point symmetry

at an anion site is C_2 , but this symmetry is reduced to C_1 by the defect at the cation site. However, it was implicitly assumed in the interpretation of the ESR absorption induced by gamma-ray irradiation that the crystal field has axial symmetry about the line joining the anion and cation sites. This is equivalent to the assumption that the field due to the charge deficiency is substantially larger than that of the normal crystal. This assumption will be seen to be only moderately well justified. We begin by considering only the effect of the axial component of the crystal field. The rhombic component is treated subsequently as a perturbation on the axial component.

The ground configuration of O^- is $1s^2 2s^2 2p^5$, with the single term 2P . With the assumption of axial symmetry, the relevant part of the crystal potential can again be replaced by the equivalent operator given in Eq. (III.5). In this instance, however, the z direction is along the line joining the anion and cation sites involved in the center. It is readily seen from Eq. (III.5) that the crystal field splits the ground term into two terms, 2PA and 2PE , with energies equal to $(\frac{2}{5})ec_{20}\langle r^2 \rangle$ and $-(\frac{1}{5})ec_{20}\langle r^2 \rangle$, respectively. Since the field is primarily due to the charge deficient cation site, which appears as an extra negative charge placed on the z axis, it can be seen from Eq. (II.2a) that c_{20} is negative and the orbital singlet, 2PA , lies lowest. Thus the only optical absorption band associated with this defect corresponds to a transition from the 2PA to the 2PE state, with energy given by

$$\Delta = \frac{3}{5}e|c_{20}|\langle r^2 \rangle. \quad (\text{V.1})$$

The quantity $\langle r^2 \rangle$ was again evaluated numerically, using a $2p$ wave function for O^- calculated by Hartree, Hartree, and Swirles,³² with the result, in atomic units,

$$\langle r^2 \rangle = 3.04. \quad (\text{V.2})$$

By Kramers' theorem,⁴³ there is no zero-field splitting of the spin degeneracy. However, the crystal field does affect the g values, which are again given by Eqs. (III.12a) and (III.12b). In this case, \parallel and \perp are with respect to the line joining the anion and cation sites. For this center, unlike the other two centers considered, there exist both ESR and optical absorption spectra. Consequently we are in a position to regard the strength of the crystal field as an adjustable parameter and to use the measured ESR spectrum to establish a correlation between the center and one of the optical absorption bands. The value of λ/Δ inferred by Gamble *et al.*³ from the ESR spectrum of gamma-irradiated Al_2O_3 was

$$\lambda/\Delta = -0.0073, \quad (\text{V.3})$$

based on the measured g values and Eqs. (III.12a) and (III.12b).

A value of the spin-orbit coupling constant λ for O^- was obtained by extrapolation from an isoelectronic sequence, as shown in Fig. 6. The λ 's for the isoelectronic

⁴⁰ A. S. Chakravarty and R. Bersohn, in *Paramagnetic Resonance*, edited by W. Low (Academic Press Inc., New York, 1963), Vol. I, p. 305.

⁴¹ D. W. Wylie, A. J. Shuskus, C. G. Young, and O. R. Gilliam, *Phys. Rev.* **125**, 451 (1962).

⁴² J. C. Slater, *Phys. Rev.* **36**, 57 (1930).

⁴³ H. A. Kramers *Proc. Acad. Sci. Amsterdam* **33**, 959 (1930).

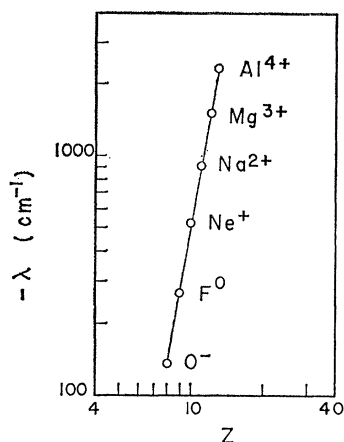


FIG. 6. Spin-orbit coupling constant versus atomic number for an isoelectronic sequence of ions. The value of λ for O^- was obtained by extrapolation.

ions were calculated from the multiplet widths in the ground term, as reported in Moore's tables.²⁸ The value of λ for O^- obtained by this procedure is -135 cm^{-1} which, together with Eq. (V.3), gives an optical absorption energy Δ of $18\,800 \text{ cm}^{-1}$ or 2.32 eV . This value is in fair agreement with the 3.08-eV band reported by Levy,¹ which is therefore ascribed to this center.

In the preceding paragraph, the strength of the crystal field was regarded as an adjustable parameter for the purpose of establishing a correlation between the ESR and optical absorptions. The crystal field due to a charge-deficient cation site has also been calculated in an effort to determine the magnitude of the charge deficiency from the observed spectra. From Eq. (II.2a), the contribution of the charge-deficient cation site to c_{20} is given by

$$c_{20} = -Ze/r_0^3, \quad (\text{V.4})$$

where Z is the magnitude of the charge deficiency, and r_0 is the anion-cation distance. The center actually occurs in two distinct arrangements with slightly different anion-cation distances depending on whether the anion and cation sites involved belong to the same molecule or adjacent molecules, as shown in Fig. 7. The distances are, respectively, 1.97 \AA and 1.86 \AA .²⁵ For the moment, we use the average value, $r_0 = 1.915 \text{ \AA}$. The charge deficiency Z can have the values 1, 2, or 3, depending on whether the defect is a divalent cation impurity, a monovalent impurity, or a vacancy, respectively. With the choice $Z=3$, Eqs. (V.1) and (V.3) give the values

$$\Delta = 2.93 \text{ eV}, \quad (\text{V.5a})$$

$$\lambda/\Delta = -0.0057. \quad (\text{V.5b})$$

Although both quantities are inferred by a graphical resolution of spectra into components, Δ is known much more precisely than λ/Δ . Thus $Z=3$ appears to give the best agreement with experiment and accordingly the defect is identified as a cation vacancy rather than an impurity.

TABLE V. Contributions of an adjacent cation vacancy to the crystal-field constants at the anion site. The constants are referred to the coordinate axes at ion 1 in Fig. 2. Headings 1 and 2 refer to arrangements 1 and 2 of Fig. 7. The units are e^2/a_r^3 .

| | 1 | 2 |
|----------|---------|---------|
| c_{20} | -16.923 | 8.275 |
| c_{21} | 0 | -23.004 |
| d_{21} | -26.277 | 14.113 |
| c_{22} | 5.978 | -5.361 |
| d_{22} | 0 | 10.548 |

Transitions between the 2PA and 2PE levels can only be induced by light polarized perpendicular to the z axis. Gamble *et al.*³ infer that the site z axes tend to be distributed more nearly perpendicular than parallel to the crystal c axis. Thus light polarized parallel to the crystal c axis should be absorbed most effectively, and the anisotropy is positive in the sense of Mitchell, Rigden, and Townsend.² This point has not yet been investigated experimentally.

When account is taken of the crystal field due to the normal lattice, which splits the orbital degeneracy of the 2PE level, and of the different values of r_0 appropriate to the two arrangements of the center, a total of four optical bands results. The contributions of the normal lattice to the crystal-field constants at the anion site are listed in Table II. The contribution of the cation vacancy can be calculated from Eq. (V.4) with $Z=3$. However, Eq. (V.4) gives the crystal-field constant appropriate to a coordinate system in which the z axis is directed from the anion site to the cation site. The corresponding constants referred to the coordinate system at ion 1 in Fig. 2 are listed in Table V.

In analogy with Eq. (III.5), the crystal potential was replaced by the equivalent operator

$$V_C = \left(\frac{1}{5}\right)e\langle r^2 \rangle \sum_i \{ c_{20} [3l_{zi}^2 - l_i(l_i + 1)] + \left(\frac{3}{2}\right)(c_{21} - id_{21})(l_+ il_{zi} + l_z il_+) + \left(\frac{3}{2}\right)(c_{21} + id_{21})(l_- il_{zi} + l_z il_-) + 3(c_{22} - id_{22})l_{+i}^2 + 3(c_{22} + id_{22})l_{-i}^2 \}, \quad (\text{V.6})$$

where c_{lm} and d_{lm} include the contributions of both the normal lattice and the adjacent cation vacancy. The matrix of V_C within the ground configuration is given in Table VI.

The matrix of V_C for each arrangement was calculated and diagonalized. The resulting optical bands occur at 2.40 and 4.59 eV in arrangement 1 and at 1.29

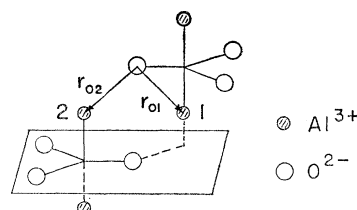


FIG. 7. Two distinct arrangements for the center consisting of an O^- ion adjacent to a charge-deficient cation site. $r_{01} = 1.97 \text{ \AA}$ and $r_{02} = 1.86 \text{ \AA}$.

TABLE VI. Matrix of V_C within the ground configuration of O^- adjacent to a cation vacancy, in units of $(1/5)(e^2/a_r^3)(r^2)$. Rows and columns are labeled by M_L .

| | 1 | 0 | -1 |
|----|---------------------------------|--------------------------------|--------------------------------|
| 1 | $-c_{20}$ | $-(3/2)(c_{21}-id_{21})$ | $-6(c_{22}-id_{22})$ |
| 0 | $-(3/\sqrt{2})(c_{21}+id_{21})$ | $2c_{20}$ | $(3/\sqrt{2})(c_{21}-id_{21})$ |
| -1 | $-6(c_{22}+id_{22})$ | $(3/\sqrt{2})(c_{21}+id_{21})$ | $-c_{20}$ |

and 3.40 eV in arrangement 2. The average of these values is 2.92 eV, in agreement with Eq. (V.5a) and with experiment. However, the spread in these values is twice the observed width of the 3.08-eV band, 1.50 eV.¹ One possibility is that the crystal field of the normal lattice is reduced by distortion, and the four bands are not resolved. Another possibility is that only the 2.40- and 3.40-eV bands should be identified with the 3.08-eV band; the 4.59-eV band may correspond to the weaker band reported by Levy at 4.28 eV,¹ and the 1.29-eV band may actually occur at less than 1 eV where no observations were made.

VI. SUMMARY

Energy levels were calculated for three trapped-hole centers in irradiated Al_2O_3 : interstitial O^0 , interstitial O^+ , and O^- adjacent to a charge-deficient cation site. Although the effect of lattice distortion about the defects was considered only qualitatively, it was nonetheless possible to draw a number of conclusions.

The absence of an ESR spectrum due to interstitial O^0 produced by reactor irradiation⁴ is accounted for by the result that, with allowance for lattice distortion, the zero-field splitting of the spin degeneracy exceeds the energy of the microwave photons employed. A single optical-absorption band at 2.0 eV¹ is attributed to interstitial O^0 and is predicted to have negative anisotropy.

A three-line ESR spectrum produced by subsequent low-temperature gamma-irradiation of reactor-irradiated crystals has been attributed to interstitial O^+ .⁴ This assignment was verified by the fact that the calculated zero-field splitting for interstitial O^+ agrees well with the corresponding spin-Hamiltonian parameter of the three-line spectrum when allowance is made for a small lattice distortion. It is further predicted that no optical-absorption bands are associated with this center.

The ESR spectrum produced by gamma irradiation includes a component which has been attributed to O^- adjacent to a charge-deficient cation site.³ On the basis of this model and the measured g values, this center was correlated with an optical absorption band at 3.08 eV.¹ A crystal-field calculation showed that the defect is a cation vacancy rather than an impurity. The optical band is predicted to have positive anisotropy.

These results tend to verify the identification of trapped-hole centers from ESR spectra, but the conclusions could be asserted with greater confidence on the basis of an *a priori* calculation of lattice distortion. Also, the remaining optical bands need to be correlated with other centers, some of which have been tentatively identified by ESR measurements.^{3,4}

ACKNOWLEDGMENTS

The authors are indebted to Professor O. R. Gilliam and to Dr. P. W. Levy, Dr. G. Vineyard, and Dr. M. Blume for helpful discussions, and to Professor J. O. Artman for a preprint of Ref. 20. The computational part of this work was carried out in the Computer Center of the University of Connecticut, which is supported in part by grant GP-1819 of the National Science Foundation. Thanks are also due to Lester Lipsky for assistance with programming.